Oncolytic Herpes Simplex Virus 1 Encoding 15-Prostaglandin Dehydrogenase Mitigates Immune Suppression and Reduces Ectopic Primary and Metastatic Breast Cancer in Mice[▽]

Jason D. Walker,[1] Inder Sehgal,[2] and Konstantin G. Kousoulas[1]*

Division of Biotechnology and Molecular Medicine and Department of Pathobiological Sciences, School of Veterinary Medicine,[1] and Department of Comparative Biomedical Sciences, School of Veterinary Medicine,[2] Louisiana State University, Baton Rouge, Louisiana 70803

Oncolytic herpes simplex virus 1 (HSV-1) viruses armed with immunomodulatory transgenes have shown potential for enhanced antitumor therapy by overcoming tumor-based immune suppression and promoting antitumor effector cell development. Previously, we reported that the new oncolytic HSV-1 virus, OncSyn (OS), engineered to fuse tumor cells, prevented tumor growth and metastasis to distal organs in the 4T1/BALB/c immunocompetent breast cancer mouse model, suggesting the elicitation of antitumor immune responses (Israyelyan et al., Hum. Gen. Ther. 18:5, 2007, and Israyelyan et al., Virol. J. 5:68, 2008). The OSV virus was constructed by deleting the OS viral host shutoff gene (*vhs*; UL41) to further attenuate the virus and permit dendritic cell activation and antigen presentation. Subsequently, the OSVP virus was constructed by inserting into the OSV viral genome a murine 15-prostaglandin dehydrogenase (15-PGDH) expression cassette, designed to constitutively express 15-PGDH upon infection. 15-PGDH is a tumor suppressor protein and the primary enzyme responsible for the degradation of prostaglandin E2 (PGE2), which is known to promote tumor development. OSVP, OSV, and OS treatment of 4T1 tumors in BALB/c mice effectively reduced primary tumor growth and inhibited metastatic development of secondary tumors. OSVP was able to significantly inhibit the development and accumulation of 4T1 metastatic tumor cells in the lungs of treated mice. *Ex vivo* analysis of immune cells following treatment showed increased inflammatory cytokine production and the presence of mature dendritic cells for the OSVP, OSV, and OS viruses. A statistically significant decrease in splenic myeloid-derived suppressor cells (MDSC) was observed only for OSVP-treated mice. These results show that intratumoral oncolytic herpes is highly immunogenic and suggest that 15-PGDH expression by OSVP enhanced the antitumor immune response initiated by viral infection of primary tumor cells, leading to reduced development of pulmonary metastases. The availability of the OSVP genome as a bacterial artificial chromosome allows for the rapid insertion of additional immunomodulatory genes that could further assist in the induction of potent antitumor immune responses against primary and metastatic tumors.

Oncolytic human herpes simplex viruses (HSV) have been genetically engineered to limit neurovirulence and the establishment of latency and reactivation and to replicate exclusively in cells with deficient apoptotic mechanisms (i.e., cancer cells) (5, 6, 37). These genetic changes are fundamental to the safety and efficacy of oncolytic herpesviruses but often result in rapid clearance of the virus by the host immune response, thus limiting its therapeutic potential. It is precisely the antiviral immune response, however, that is thought to help overcome tumor-induced immune suppression, allowing for antitumor immunity to develop. In this regard, HSV-1 infections within tumors may function as *in situ* vaccines, providing the necessary inflammatory signals that engage innate and adaptive immune responses to tumor antigens. Thus, oncolytic HSV-1 may be effective both directly as a cancer killing agent and indirectly as an immunological enhancer, or *in situ* cancer vaccine (13, 49). Previously, we reported that the novel fusogenic oncolytic

herpesvirus OncSyn (OS) was effective at treating primary solid breast tumors in mice (25, 26). Moreover, treatment of primary 4T1 tumors in syngeneic BALB/c mice with OS led to a substantial reduction in the formation of metastatic foci within multiple organs and in some cases eliminated lung metastasis, suggesting the development of effective antitumor immunity (43).

The HSV-1 *vhs* gene product encoded by the UL41 open reading frame (ORF) has multiple functions that are known to suppress antiviral immune responses. (i) *vhs* is an RNase that degrades viral and cellular mRNAs, limiting host and viral antigen production (3, 32, 33, 45, 48, 51, 56, 59, 61, 65, 75). (ii) UL41 (*vhs*) with ICP47 is known to inhibit major histocompatibility complex I (MHC-I) antigen presentation (59), while *vhs* alone has also been implicated in the reduction of MHC-II expression (69). (iii) *vhs* has been reported to suppress production of cytokines and chemokines and inactivate dendritic cells (7, 59). In agreement with these reports, deletion of the *vhs* gene prevented HSV-1-mediated inactivation of antigen presentation by dendritic cells (DC) (54) and improved the immunogenicity of a candidate replication-defective HSV-1 vaccine strain (16, 55). Furthermore, deletion of the *vhs* gene causes substantial reduction in neurovirulence (48, 60, 64).

* Corresponding author. Mailing address: Division of Biotechnology and Molecular Medicine and Department of Pathobiological Sciences, School of Veterinary Medicine, Louisiana State University, Baton Rouge, LA 70803. Phone: (225) 578-9682. Fax: (225) 578-9701. E-mail: vtgusk@lsu.edu.

It is generally assumed that advanced tumors promote the formation of an immunosuppressive and tolerogenic microenvironment that subverts the innate immune response, leading to the inhibition of antitumor adaptive immune responses (14, 46, 76). Tumor-derived immunomodulation may include alteration of tumor antigen expression to render tumor cells less detectable by the immune system, secretion of factors and cytokines that inhibit dendritic and T cell functions, and induction of immune cells that can suppress antitumor immune responses, including myeloid suppressor cells (MDSC) and regulatory T cells (Treg) (44).

A prominent immunosuppressive factor in many cancers is prostaglandin E2 (PGE2). PGE2 is a short-lived lipid-based signaling molecule with potent localized paracrine and autocrine functions that is particularly important for tumor development. PGE2 has been shown to promote tumor angiogenesis (38, 71), drug resistance (36), invasion and migration (35), immune suppression (24, 72, 73), and the inhibition of apoptosis (34). PGE2 is generated by tumors and tumor-associated immune cells from arachidonic acid, with the rate-limiting step being the enzymatic activity of cyclo-oxygenase 2 (COX-2). PGE2 is negatively regulated by rapid conversion to 15-keto metabolites by 15-prostaglandin dehydrogenase (PGDH), an enzyme with both intra- and extracellular functions. Not surprisingly, 15-PGDH is a tumor suppressor (2, 9, 42, 74), and loss of 15-PGDH expression in a variety of cancers often accompanies COX-2 upregulation and can be correlated with disease progression (2, 35, 66, 67, 70). Elevated levels of tumor-associated COX-2, coupled with a loss of PGDH expression, allows many tumors to maintain high levels of PGE2, which is a poor prognostic indicator and is considered to be an important step in the evolution of malignant cancers (reviewed in reference 21). COX-2 activity in tumors may be blocked using selective or nonselective inhibitors whose use has been shown to significantly decrease cancer risk for a wide range of cancer types (reviewed in references 22 and 23, respectively); however, systemic COX-2 inhibition has side effects that are poorly tolerated. Transient localized restoration of PGDH expression in tumors using targeted adenoviral vectors has been shown to inhibit PGE2 accumulation and tumor angiogenesis and growth (27). Overall, tumor-associated PGE2 is strongly associated with immune suppression and cancer progression. Novel anticancer immune therapies designed to limit PGE2 signaling could promote stronger immune responses and inhibit tumor development.

In the present study, we have constructed and characterized a third-generation recombinant oncolytic viral vector (OSVP) designed to be more immunogenic than the parental OS virus due largely to deletion of the viral host shutoff (*vhs*) gene. Furthermore, we constructed the OSVP virus to constitutively express 15-PGDH, the principal enzyme responsible for degradation of PGE2. We show that infection of 4T1 breast tumors implanted in syngeneic and immunocompetent BALB/c mice with OSVP inhibits metastasis, triggers substantial inflammatory cytokine production, and promotes antitumor immune responsiveness.

MATERIALS AND METHODS

Cells. African green monkey kidney (Vero) cells and mouse mammary tumor cells (4T1) (1) were obtained from the American Type Culture Collection (Ma-

nassas, VA). Vero cells were maintained in Dulbecco's modified Eagle's medium supplemented with 10% fetal calf serum (FCS) and antibiotics. 4T1 cells and primary mouse cells were maintained in RPMI 1640 medium containing 10% FCS (Invitrogen, Carlsbad CA). The cultures were maintained at 37°C in a humidified atmosphere of 5% CO_2.

Construction of recombinant OSV and OSVP viruses. The previously published OS viral genome recovered as a bacterial artificial chromosome (BAC) in *Escherichia coli* (pOS) (26) was used for the construction of the pOSV BAC plasmid. The coding region of UL41 (nucleotides 91111 to 92638) was deleted to yield pOSV using double-red mutagenesis in *E. coli* (68). The OSV virus was recovered after transfection of Vero cells with pOSV. pOSVP was generated from pOSV by inserting an ~3.1-kbp gene expression cassette containing the *Mus 15-musculus* hydroxyprostaglandin dehydrogenase (15-NAD) cDNA (cDNA clone MGC:14001 IMAGE:4208980) under the control of the human cytomegalovirus immediate-early HCMV IE promoter. The inserted gene cassette includes nucleotide sequences beginning 12 nucleotides proximal to the ClaI restriction site and extending to 7 nucleotides before the NsiI restriction site of the 15-NAD gene. This fragment was inserted into the locus previously occupied by UL41, in the same genomic orientation as UL41 (right to left). The OSVP virus was recovered after transfection of Vero cells with pOSVP. These modifications were confirmed by restriction enzyme and DNA sequence analyses of the affected genomic regions.

Phenotypic characterization and replication kinetics of the OSV and OSVP viruses. Cells (both Vero and 4T1) were seeded into 6-well plates and infected the following day (when they had reached approximately 95% confluence) with either the HSV-1(F) strain, OS, OSV, or OSVP at a multiplicity of infection (MOI) ranging from 0.001 to 1 PFU/cell. Cells were cultured in a maintenance medium (containing 2% FCS) and were left for 2 days to allow for cytopathic effects to develop. Infected cells were visualized by immunohistochemistry at 48 h postinfection (h.p.i.) using horseradish peroxidase-conjugated anti-HSV antibody (Dako, Carpinteria, CA) and the Novared substrate development kit (VectorLabs, Burlingame, CA). Images were captured using phase-contrast microscopy, as reported previously (26).

To determine the replication kinetics of the viruses, one-step growth kinetics and viral titers at 48 h.p.i. were determined as described previously (11, 12). Briefly, nearly confluent monolayers of either Vero or 4T1 cells were infected with each virus at an MOI of 5 at 4°C for 1 h. Thereafter, virus was allowed to penetrate for 2 h at 37°C. Any remaining extracellular virus was inactivated by low-pH treatment with phosphate-buffered saline (PBS) at pH 3.0. Supernatants were harvested at given time points following normal culture conditions, and viral titers were obtained by endpoint titration on Vero cells.

15-PGDH activity. Transfection of Vero cells with the 15-PGDH mammalian expression vector was achieved using Lipofectamine 2000 (Invitrogen) according to the manufacturer's suggested protocol. Cell culture supernatant PGE2 levels were determined by enzyme-linked immunosorbent assay (ELISA) using Prostaglandin E_2 Express EIA kits (Cayman Chemical, Ann Arbor, MI).

4T1 BALB/c tumor growth and pulmonary metastasis determinations. Female BALB/c mice were obtained from Charles River (Wilmington, MA) and housed in an animal room which was kept at 25°C with a 12-h light-dark cycle. All experimental procedures involving animals were approved by the institutional animal care and use committee (IACUC) of the Louisiana State University. At 6 to 7 weeks of age, 1×10^5 viable 4T1 cells suspended in 0.1 ml of PBS with 20% growth factor reduced Matrigel (BD Biosciences, Franklin Lakes, NJ) were implanted subcutaneously in the interscapular area of the animals by the use of a 27-gauge needle. Tumor sizes were monitored beginning ~7 days after tumor inoculation by direct measuring with a digital microcaliper. Tumor volumes were calculated using the following formula: volume = (length × width × height)/2, as reported previously (26). At an average tumor volume of approximately 200 mm³ (12 days post-tumor inoculation), animals were randomized into 4 groups. The groups of mice received 3 intratumoral injections of the OS, OSV, or OSVP viral particles or PBS every 4 days. Virus was prepared by brief centrifugation to clear cellular debris and diluted to the appropriate concentration of PFU using PBS. Each tumor was injected with approximately 1×10^7 PFU per injection in a 0.1-ml volume, while control mice received PBS. Injections were performed slowly at 2 different sites per tumor. Heat inactivation of virus was achieved by incubation at 95°C for 20 min.

For pulmonary metastatic burden assays, tumor-bearing mice treated as above were euthanized with CO_2 at days 29 to 30 post-tumor inoculation. Lungs from each mouse were excised, minced, and digested for 75 min at 4°C while rocking in buffer containing elastase and collagenase type IV. Following filtration through a 100-μm nylon screen, total lung homogenates for each mouse were serially diluted and cultured for 1 week in RPMI 1640 with 10% FBS and 60 μM 6-thioguanine. 6-Thioguanine-resistant colonies were formalin fixed and stained
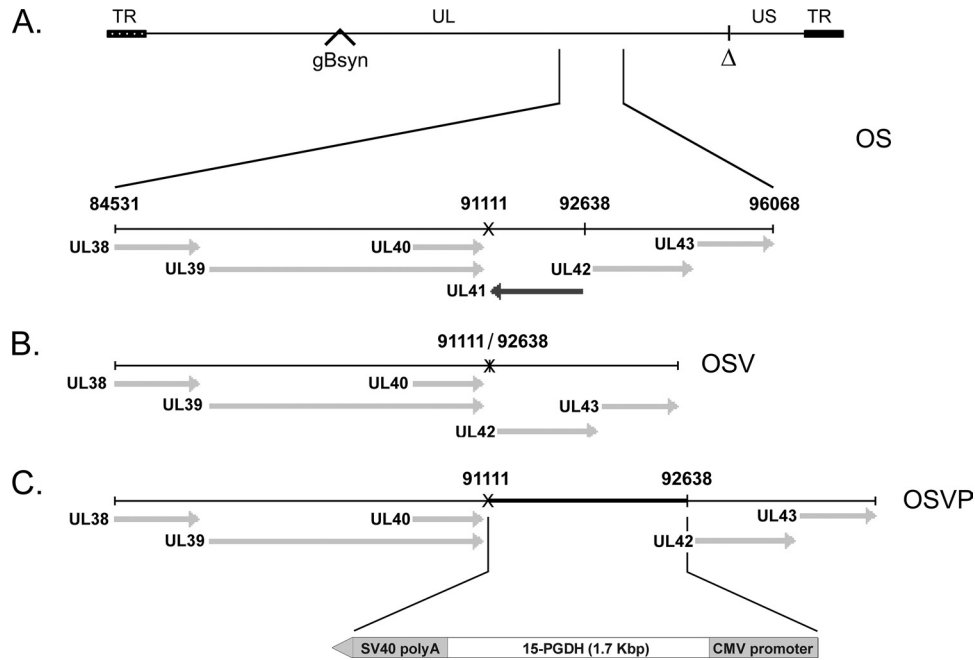
FIG. 1. Schematic representation of the genomic structure of oncolytic recombinant viruses OSV and OSVP. (A) Representation of the prototypic arrangement of the HSV-1 OncSyn (OS) genome with the unique long (UL) and unique short (US) regions flanked by the terminal repeat (TR) regions. The Δ denotes the approximate location of the OS genomic deletion between the UL and US regions (26), and the position of the gB syncytial mutation is indicated. The expanded area below the depicted genome shows the genomic region from 84531 to 96068 nucleotides encompassing the UL38-UL43 genes. (B) Genomic organization of the OSV recombinant virus showing deletion of the UL41 gene. (C) Genomic organization of the OSVP recombinant virus showing insertion of the 15-PGDH gene cassette in place of the deleted UL41 sequences. SV40, simian virus 40.

with crystal violet for visualization and counting. Stained colonies with >20 cells were counted, with each colony representing one clonogenic metastatic cell (50).

Immunophenotyping of mouse splenocytes and lymphocytes. All analyses were conducted using freshly harvested splenocytes or by draining lymph node cells from animals with similarly sized tumors (150 ± 25 mm³). Animals were treated twice (day 1 and day 4) with PBS, OS, OSV, or OSVP, and spleens and draining lymph nodes were harvested on day 5. The organs were manually dissociated in RPMI and filtered through a 100-μm nylon mesh. Erythrocytes were removed by 5-min exposure to ACK (150 mM NH_4Cl, 0.1 mM EDTA, 10 mM $KHCO_3$; pH 7.3) lysing buffer. Cells for flow cytometry were surface labeled with fluorescently conjugated antibodies to either murine CD83 (catalog number 558205, BD Biosciences) to identify activated lymphocytes and dendritic cells, or CD11b and Gr-1 (catalog numbers 552850 and 553126, respectively; BD Biosciences) to identify MDSC. Species-appropriate isotype control antibody conjugates were used in each experiment to identify positive populations (catalog numbers 554685, 552849, and 556923, respectively; BD Biosciences). Regulatory T cells (Treg) were labeled using the mouse Treg flow kit from Biolegend, San Diego, CA (catalog number 320015), according to the manufacturer's instructions. All cytometric datum acquisition was performed on a FACScalibur instrument (BD Biosciences) and analyzed using WinMDI flow cytometry analysis freeware (written by Joseph Trotter, The Scripps Research Institute, La Jolla, CA).

For ex vivo effector cytokine production analyses, splenocytes were cultured ex vivo in a 96-well format in either control or anti-mouse CD3-coated tissue culture plates (both from BD Biosciences, catalog numbers 354720 and 354730) in triplicate at a density of 100,000 cells per well. Supernatants were harvested after 24-h incubation and analyzed for murine Th1 and Th2 cytokine production (Bio-Plex Pro Mouse cytokine TH1/TH2 assay catalog number M60-00003J7; Bio-Rad, Hercules, CA).

Statistical analyses. Unless otherwise indicated, Student's t test was used to determine P values and establish significant differences for sample means ($P < 0.05$). Tumor growth curve analyses used a distribution-free test established for tumor growth curve comparisons (31). Pulmonary 4T1 metastatic burden comparisons were conducted using the Mann-Whitney nonparametric statistical hypothesis test ($P < 0.05$, one tailed) supplied on GraphPad software (GraphPad Software, Inc., La Jolla, CA).

RESULTS

Construction and characterization of HSV-1 OSVP. The recombinant viruses OSV and OSVP were constructed by double-red mutagenesis of the HSV OS genome cloned into a bacterial artificial chromosome (BAC) (26). The OS viral genome lacks a section of the HSV-1 large inverted repeat region encompassing a single copy each of the ICP0, γ34.5, and ICP4 genes. This region was replaced by a gene cassette constitutively expressing the red fluorescence protein (RFP; HcRed) under the eukaryotic translation elongation factor 1-a promoter control. In addition, the OS genome contains the gBsyn3 syncytial mutation that causes extensive virus-induced cell fusion (Fig. 1A) (25, 26). The double-red recombination method (68) was utilized to delete the entire UL41 ORF (vhs) of the OS BAC (bOS) to produce the OSV BAC (bOSV) and OSV virus, as described in Materials and Methods (Fig. 1B). The bOSV genome was used for a subsequent round of double-red recombination in which a gene cassette containing the murine 15-PGDH under the control of a CMV promoter was inserted into the vhs deletion site. The resulting bOSVP genome was transfected into Vero cells to recover the OSVP virus (Fig. 1C). The genotypes of OSV and OSVP viral genomes were confirmed by direct DNA sequencing (see Materials and Methods).

The replication and average plaque morphology characteristics of the OSV and OSVP viruses were compared to those of their parental virus OS and the prototypic HSV-1(F) strain used to derive the OS virus in cell culture experiments (Fig. 2A). The OS virus produced syncytial plaques that were, on the
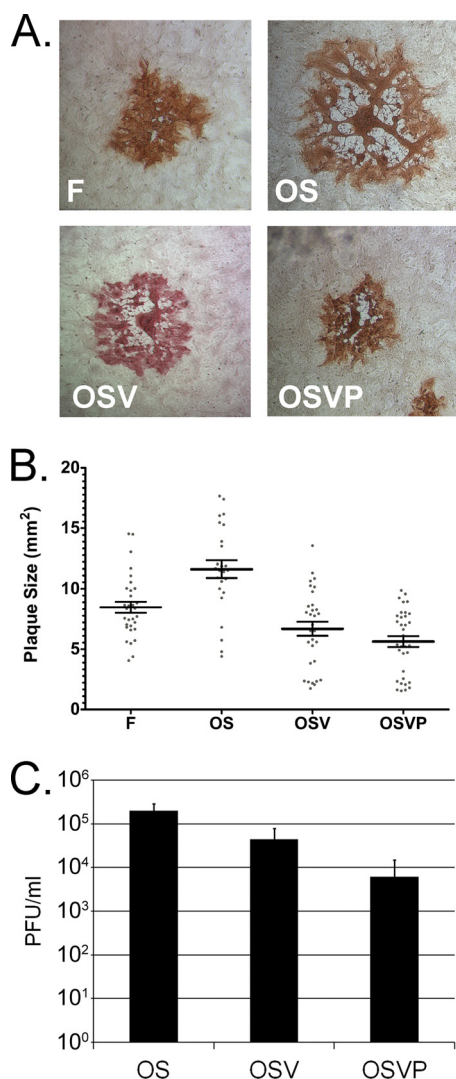
FIG. 2. Plaque morphology and growth characteristics of OS OSV and OSVP. (A) Nearly confluent Vero cell monolayers were infected with wild-type HSV-1(F), OS, OSV, or OSVP viruses at MOI of 0.001. Individual viral plaques were visualized 48 h postinfection by immunohistochemistry and photographed at the same magnification with a phase-contrast microscope. (B) A minimum of 30 plaques for each virus (prepared as described in the legend to panel A) were measured, and individual plaque sizes are indicated on the x axis, with the horizontal bar indicating the means for each group. Error bars indicate standard error of the means. All pairwise comparisons of the means using two-tailed t tests indicated significance ($P < 0.0185$) except for the comparison between OSV and OSVP ($P = 0.1473$). (C) Nearly confluent 4T1 cell monolayers were infected with the above-mentioned viruses at an MOI of 5. Triplicate culture supernatants were collected at 48 hpi, and viral titers were determined (PFU/ml).
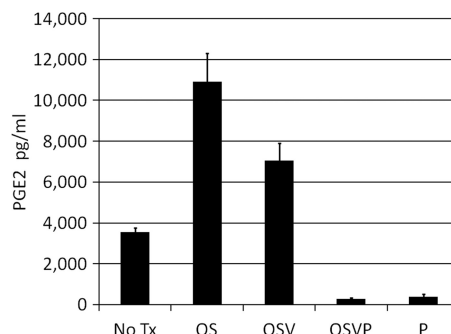

FIG. 3. PGE2 degradation by OSVP. Nearly confluent monolayers of 4T1 cells were infected with the indicated viruses at an MOI of 5. After 2 days culture supernatants were harvested and assayed for PGE2 by ELISA. P denotes transient expression with a 15-PGDH mammalian expression vector, while "No Tx" denotes mock-treated cells. PGE2 assays were performed in triplicates, and error bars represent the 95% confidence interval (CI) of the mean.

fusion, especially in high-MOI infections of Vero cell monolayers (data not shown).

The ability of the OS, OSV, and OSVP viruses to replicate in 4T1 cells was examined by determining viral titers obtained at 48 h.p.i. with an MOI of 5 (Fig. 2B). OSVP produced viral titers that were approximately one log lower than the OSV virus, while OSV produced intermediate titers approximately 5-fold lower than those of the OS virus. Additional experiments in Vero cells revealed a similar virus production pattern, with OSVP producing consistently approximately one log less virus than the OS virus (not shown).

OSVP inhibits PGE2 accumulation. To evaluate the ability of the OSVP virus to produce functional 15-PGDH, 4T1 cells were infected with OSVP virus at an MOI of 5, and 48-h.p.i. supernatants of the infected cells were collected and assayed for cumulative levels of PGE2. 4T1 cells infected with OSVP or transfected with the 15-PGDH expression vector alone displayed significantly reduced levels of supernatant PGE2 relative to the no-treatment control (>10-fold). In contrast, infection with OS or OSV resulted in remarkable increases in supernatant PGE2 (Fig. 3).

OSV and OSVP inhibit 4T1 tumor growth. Previously, we showed that treatment of 4T1 tumors in immunocompetent BALB/c mice with the OS virus resulted in substantial reduction in tumor growth and metastasis to the lungs and other organs (26). Similar experiments were performed to assess the relative abilities of the OSV and OSVP virus to inhibit 4T1 tumors. Mice bearing palpable tumors were treated with four doses of virus (1×10^7 PFU/dose) injected intratumorally at 3-day intervals (Fig. 4). Mice treated similarly with PBS served as negative controls. Separate experiments using heat-inactivated OSVP and UV-inactivated OS failed to reduce tumor growth compared with PBS controls (data not shown; 26). Tumor measurements were collected until the mice were sacrificed at day 20 (posttreatment). All three viruses, OS, OSV, and OSVP, resulted in similar reductions of tumor growth (Fig. 4).

OSV and OSVP treatments reduce the incidence of pulmonary metastases. Previously, we showed that OS treatment of 4T1 tumors in BALB/c mice reduced the incidence of tumor
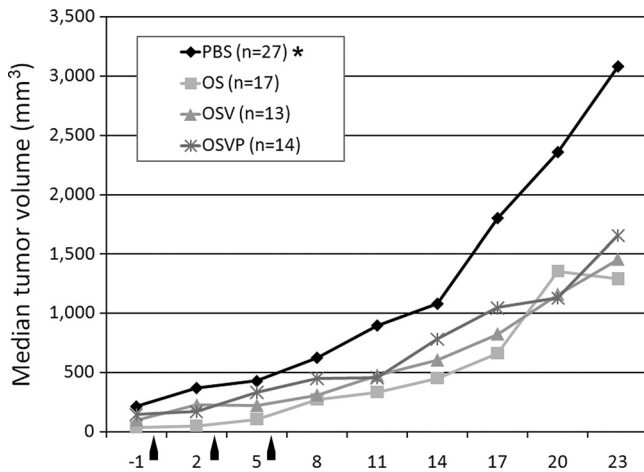
average, larger than those of the prototypic HSV-1(F) at 48 h.p.i. Deletion of the UL41 gene did not appreciably affect plaque morphology of the resultant OSV virus, in as much as the viral plaques remained syncytial and OSVP produced plaques of sizes similar to those produced by the OS virus (Fig. 2B). Both OSV and OSVP produced strong syncytial plaque phenotypes (Fig. 2A) and caused extensive virus-induced cell

FIG. 4. Intratumor treatment with OS, OSV, or OSVP viruses. A total of 1×10^5 viable 4T1 cells were implanted subcutaneously in the interscapular area of BALB/c mice. Tumors were measured using a digital caliper at defined time intervals prior to and after treatment (x axis). Median tumor volumes over time are shown on the y axis. Tumors were injected with each virus (1×10^7 PFU/ml in PBS buffer), or PBS alone when tumors reached approximately 80 to 90 mm^3 in volume. Tumor volumes were measured prior to (negative values on the x axis) and after the injections. Tumors were treated with each virus at days 1, 3, and 6, as indicated by arrows. The asterisk indicates statistical significance by nonparametric analysis (31). The results shown are from one of three independent experiments that produced similar results.
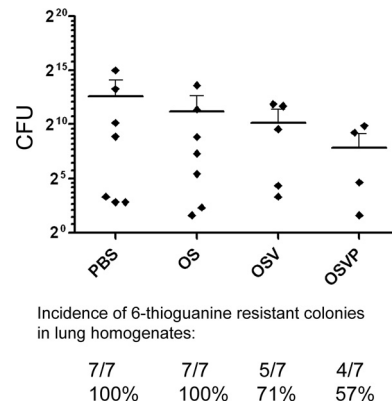

FIG. 5. Quantification of pulmonary metastases. Virus-treated mice bearing 4T1 tumors were sacrificed 30 days post-tumor inoculation, and both lungs were harvested from each treated mouse and homogenized for cell culture. Clonogenic metastatic foci derived from total lung homogenates were enumerated by limited dilution culture in the presence of 6-thioguanine. Individual resistant colonies were counted and used to determine the number of CFU per animal (x axis). Shown are the calculated CFU of each mouse sorted by treatment. Means for each treatment group are represented by horizontal bars with error bars delineating 95% CI. The mean number of metastatic colonies recovered from the OSVP-treated group was significantly less than that of the PBS control group (Mann-Whitney test; $P = 0.0474$), but other pairwise comparisons did not prove statistically significant. The results shown are from one of three independent experiments that produced similar results. Not all samples yielded colonies, and the ability to recover colonies was used to determine pulmonary metastasis incidence rates for each group (shown below the chart).

metastases (25). To determine the abilities of OSV and OSVP viruses to inhibit development of tumor metastasis, pulmonary metastatic loads in treated and untreated animals were assessed 30 days post-tumor inoculation, by determining the number of 6-thioguanine-resistant clonogenic 4T1 cells recoverable from total lung homogenates per mouse (see Materials and Methods). OSVP treatment significantly reduced the number of recovered pulmonary clonogenic 4T1 cells in comparison to the PBS-treated control. Furthermore, OSVP also reduced the overall incidence of pulmonary metastasis as determined by the ability to recover clonogenic 6-thioguanine-resistant cells (Fig. 5). OS and OSV treatments resulted in intermediate but not statistically significant reductions in metastatic pulmonary tumors in comparison to PBS, but only OSV was able to reduce the incidence of pulmonary metastasis, similar to OSVP. A pairwise comparison of OSV and OSVP treatments was unable to establish statistically significant differences in metastasis or incidence.

OSVP alleviates PGE2-based immune suppression in mice with advanced 4T1 tumors. PGE2 promotes the development and activity of immunosuppressive cell populations, including MDSC and Treg (53, 57, 58). To examine the effect of 15-PGDH expression and the expected PGE2 reduction of immune suppression in mice treated with the OSVP virus, the relative proportions of splenocytes and lymphocytes of lymph node origin possessing suppressor cell phenotypes were determined by polychromatic flow cytometry. OSVP-treated mice exhibited a significant decrease in splenic MDSC compared to OSV (Fig. 6A). In contrast, splenic Treg were not significantly reduced (data not shown), although oncolytic therapy alone appeared sufficient to inhibit some Treg accumulation in lym-

phocytes from lymph nodes (Fig. 6B). Elevated PGE2 has been shown to inhibit dendritic cell maturation (20). The proportions of CD83-positive cells (representing mature DC and activated T cells) present in spleens from OSVP-treated mice were significantly increased relative to PBS-, OS-, or OSV-treated controls (Fig. 6C). Similarly, CD83$^+$ lymphocytes were significantly increased in OSVP-treated animals in comparison to PBS-, OS-, and OSV-treated controls (Fig. 6D).

Th1/Th2 cytokine profiling was performed to assess the baseline and stimulated immune activities of splenocytes from treated and control mice bearing similar-size tumors. Generally, OS, OSV, and OSVP viruses appeared to stimulate unbiased effector helper T cell activity, as evidenced by the production of similar levels of Th1 (interleukin 2 [IL-2], granulocyte-macrophage colony-stimulating factor [GM-CSF], and gamma interferon [IFN-γ]) and Th2 (IL-5, IL-4, IL-10, and IL-12) cytokines in comparison to those of the PBS-treated control animals (Fig. 7A). Polyclonal stimulation of isolated splenocytes with immobilized CD3 antibody produced a pattern of immune stimulation similar to that of unstimulated splenocytes, with the exception that a significantly more robust production of the relevant cytokines was observed in comparison to that of PBS-treated animals (Fig. 7B).

DISCUSSION

We have previously reported that the oncolytic HSV-1(F)-based virus OS inhibited primary tumor growth and the formation of metastatic tumors in the 4T1/BALB/c immunocompetent mouse system (25, 26). We sought to arm OS with the
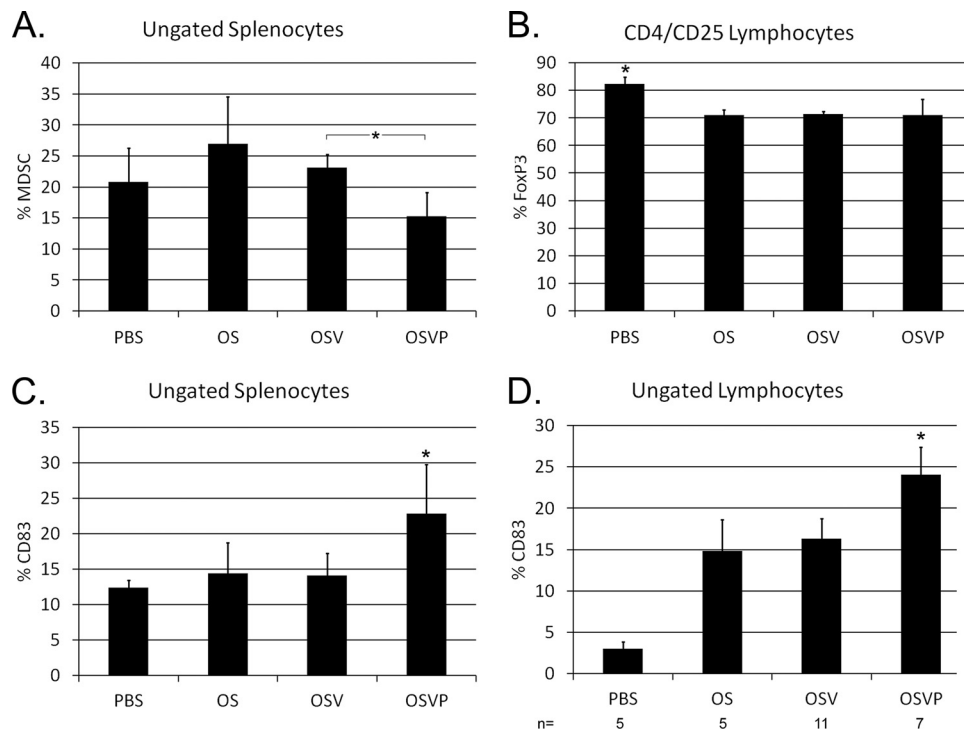
FIG. 6. Immunophenotypes of draining lymph node lymphocytes and splenocytes. 4T1 tumor-bearing mice with similarly sized and well-developed tumors were given a single intratumoral injection of the indicated viruses. After 2 days, cells from draining lymph nodes (B and D) or spleens (A and C) were isolated and analyzed for MDSC markers (Gr1$^+$, CD11b$^+$) (A), CD4+CD25+FoxP3+ regulatory T cells (B), and CD83 (C and D). Indicated phenotypes are shown as the mean percentage of total live cells interrogated by flow cytometry (error bars represent 95% CI of the means) ($n = 3$ unless otherwise noted). Asterisks with brackets indicate pairwise statistical significance. Asterisks alone indicate statistical significance over all pairwise comparisons among the treatments (two-tailed t test; $P < 0.05$).

ability to enhance potential antitumor immune responses initiated by treatment of ectopic tumors with OS. To this end, the OS virus was modified to increase antigen presentation and viral safety by deleting the *vhs* (UL41) gene. In addition, OS was modified to constitutively express 15-PGDH, causing a reduction of PGE2 accumulation and a concomitant reduction in the number of MDSC. The resultant OSVP virus showed enhanced abilities to reduce tumor growth and metastasis in the 4T1/BALB/c breast cancer mouse model system.

Characteristics of OSV and OSVP oncolytic viruses. Deletion of the *vhs* gene did not drastically affect virus replication in Vero or mouse 4T1 cells or virus-induced cell fusion caused by the gBsyn3 syncytial mutation of the parental OS virus. This result is in agreement with previous findings that deletion of the UL41 gene had modest effects on HSV-1 replication in cell culture (51, 52). The *vhs*-deleted OSV genome contains an approximately 11-kbp deletion encompassing the unique long (UL)-unique short (US) junction (25, 26) and the UL41 (*vhs*) deletion (2.5 kbp), for a total of approximately 13.5-kbp deleted sequences. Therefore, this virus is amenable to insertion of multiple gene cassettes expressing genes of interest to cancer therapy, without exceeding viral DNA packaging limits.

The 15-PGDH gene cassette was inserted in place of the *vhs* deletion on the OSV viral genome cloned as a bacterial artificial chromosome (BAC). The OSVP-BAC (bOSVP) was stable in *E. coli* and did not contain any unintended genetic alterations, as evidenced by restriction endonuclease analysis and DNA sequencing (not shown). The OSVP virus appeared

to replicate less efficiently (5-fold less) than either the OS and OSV viruses, although the syncytial phenotype of the virus was unaffected. Early work has shown that activation of latent HSV is usually associated with a local or systemic rise in prostaglandins, including PGE2. Furthermore, exogenously added PGE2 enhanced viral replication, while indomethacin, a nonsteroidal anti-inflammatory drug that inhibits PGE2, inhibited viral replication (19, 30). The mechanism by which PGE2 facilitates viral replication and egress is not known. Attempts to rescue the observed reduction in the viral replication defect of OSVP virus by adding PGE2 to infected cell cultures failed to increase viral titers (not shown). It is possible that high levels of intracellular 15-PGDH expression causes substantial reduction in intracellular PGE2 levels even in the presence of exogenously added PGE2. Typically, PGE2 levels are highly elevated within tumors, potentially promoting viral replication (17). Expression of 15-PGDH by OSVP is expected to decrease intratumoral PGE2 levels, potentially resulting in lower viral growth. However, 15-PGDH expression did not drastically reduce viral replication in cell culture (Fig. 2) or within tumors (not shown), suggesting that basal levels of PGE2 remaining in tumors after PGDH expression are sufficient for viral replication.

A critical consideration in the use of oncolytic herpesviruses in human cancer therapy is the provision for multiple safety measures against uncontrolled propagation of the virus in the host. The parental OS virus carries a large deletion encompassing the UL-US junction and containing one copy of the
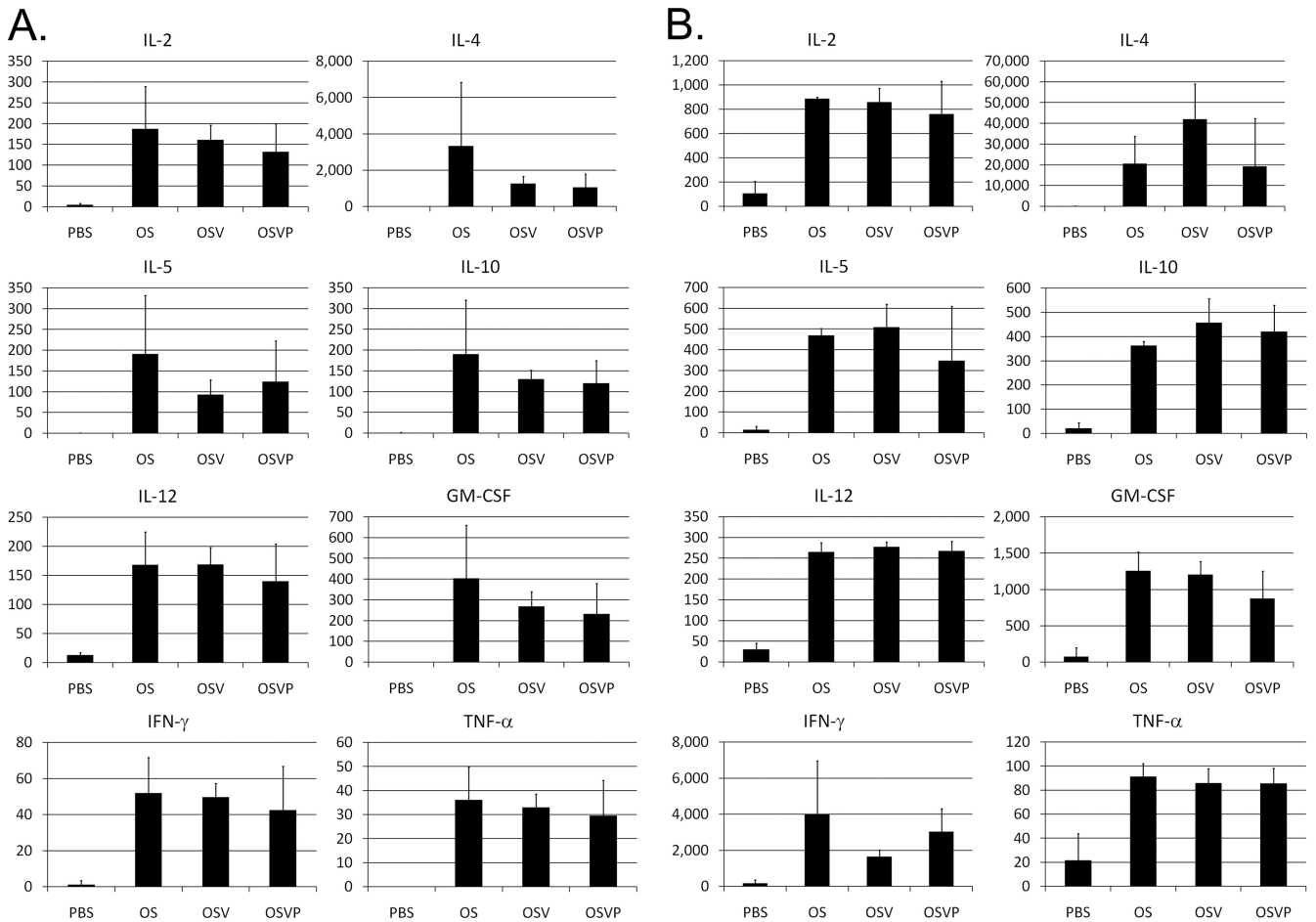
FIG. 7. Cytokine immunoprofiles of lymphocytes derived from treated mice. Mice with similarly sized 4T1 tumors (200 to 300 mm^2) were treated twice with a 3-day interval. Two days following treatments with OS, OSV, OSVP, or PBS (control), lymphocytes from draining lymph nodes were isolated and cultured for 24 h alone (A) or with immobilized anti-CD3 stimulatory antibody (B) at a concentration of 100,000 cells per ml. TNF-α, tumor necrosis factor alpha. Supernatants were assayed for TH1/TH2 cytokine production by Bioplex (Bio-Rad). Shown are the mean quantities of the indicated cytokines in pg/ml with error bars representing 95% CI ($n = 3$). Shown are results from one of two experiments with similar results.

ICP34.5 gene, as well as the immediate-early ICP0 and ICP4 genes and one of the two LAT gene loci in the viral genome (25, 26). This deletion is similar to the deletion carried by the NV1020 virus that has been tested extensively in preclinical animal models and recently in human studies, showing a high safety profile (4, 8, 15, 18, 25, 26, 28, 29). The vhs gene is known to be critically important for viral pathogenesis. Specifically, deletion of the vhs gene substantially reduced the ability of the virus to grow in trigeminal ganglia, brains, and corneas. Furthermore, vhs-deleted viruses failed to cause clinical disease and to establish and reactivate from latency (62–64). Therefore, deletion of the vhs gene provides for a significant increase in viral attenuation and safety. The production of 15-PGDH may also provide for an additional level of safety, since high levels of PGE2 increase viral replication, virus spread, and reactivation from latency (19, 30).

OS, OSV, and OSVP viruses stimulate broad immune responses. Th1/Th2 cytokine profiling revealed that all three viruses stimulated the production of similar levels of both Th1 (IL-2, GM-CSF, and IFN-γ) and Th2 (IL-5, IL-4, IL-10, and IL-12) cytokines. These results suggest that although the absence of the vhs protein and constitutive expression of 15-PGDH may directly or indirectly affect dendritic cell functions and maturation, these effects did not appreciably alter the potent local and systemic immunostimulatory properties of these viruses. Moreover the cellular responses to polyclonal T cell activation were considerably enhanced in treated animals. The presence of increased CD83-positive cells in draining lymph nodes of OSVP-treated tumors suggests that OSVP may provide additional immune enhancement. This robust immune stimulation may provide, or allow, the necessary inflammatory signals, which are known to be critical for the generation of antitumor immune responses (39–41). Importantly, the lack of the vhs gene may allow increased expression of tumor-associated antigens (TAA) into the tumor microenvironment for uptake by dendritic cells, leading to adaptive T cell priming. On the other hand, 15-PGDH expression may help ensure the overall viability of dendritic cells for optimum TAA presentation by dendritic and other professional antigen-presenting cells.

OSVP, but not OS or OSV, viruses reduce levels of MDSC and increase CD83. CD11b and GR-1 double-positive cells (MDSC) and Treg, indicated by CD3, FoxP3, and CD25 staining, represent a diverse population of PGE2-sensitive immune cells with suppressor functions that are induced by many cancers, including 4T1 (reviewed in reference 47). The OSVP virus substantially reduced the relative numbers of MDSC in treated animals in comparison to either OS or OSV viruses, suggesting that the observed MDSC inhibition was caused by the 15-PGDH expression and the concomitant reduction in PGE2 levels. The observed MDSC reduction in peripheral lymphocyte and splenocyte populations suggests that intratumoral expression of 15-PGDH is capable of producing systemic reduction of MDSC. At the same time we observed a significant increase in CD83^{+} immune cells in response to 15-PGDH, suggesting that OSVP reduces immune suppression and increases immune activation in part through 15-PGDH expression. Similar results have been obtained after adenovirus-mediated delivery of 15-PGDH in CT-26 colon carcinomas implanted in mice. This work showed not only a reduction of MDSC, but also the differentiation of intratumoral CD11b cells from immunosuppressive phenotypes to MHC class II-positive myeloid APCs (10).

OSVP treatment of highly metastatic 4T1 mouse breast tumors resulted in a substantial reduction of metastasis to mouse lungs. Additional work, however, is needed to determine the relative contributions of the *vhs* deletion and 15-PGDH insertion to this reduction. Nevertheless, others have also reported on the therapeutic effects of 15-PGDH expression in similar experiments using an adenovirus expressing murine 15-PGDH to treat murine colorectal tumors. In this system, treated mice developed antitumor immune responses that caused eradication and long-term survival in 70% of the mice (10). Unlike the adenovirus vector, the OSVP oncolytic vector platform holds particular promise for cancer therapy because it can accommodate the simultaneous expression of additional genes that can stimulate antitumor immune responses and alter the immunosuppressive milieu in the tumor microenvironment. In addition, the virus can accommodate the heterologous expression of specific TAA that can potentially augment antigen-specific antitumor immune responses. Recently, the NV1020 oncolytic virus, which represents a genomic arrangement similar to that of the OSVP virus, with the exception of the *vhs* deletion and constitutive expression of 15-PGDH, was shown to be safe and efficacious in an expanded phase I/II trial for the treatment of colorectal metastasis to the liver (15). Similarly, the true potential of the OSVP virus for cancer treatment has to be demonstrated in human clinical trials.

REFERENCES

1. **Aslakson, C. J., and F. R. Miller.** 1992. Selective events in the metastatic process defined by analysis of the sequential dissemination of subpopulations of a mouse mammary tumor. Cancer Res. **52:**1399–1405.
2. **Backlund, M. G., et al.** 2005. 15-Hydroxyprostaglandin dehydrogenase is down-regulated in colorectal cancer. J. Biol. Chem. **280:**3217–3223.
3. **Becker, Y., E. Tavor, Y. Asher, C. Berkowitz, and M. Moyal.** 1993. Effect of herpes simplex virus type-1 UL41 gene on the stability of mRNA from the cellular genes: beta-actin, fibronectin, glucose transporter-1, and docking protein, and on virus intraperitoneal pathogenicity to newborn mice. Virus Genes **7:**133–143.
4. **Bennett, J. J., et al.** 2002. Comparison of safety, delivery, and efficacy of two oncolytic herpes viruses (G207 and NV1020) for peritoneal cancer. Cancer Gene Ther. **9:**935–945.
5. **Chou, J., E. R. Kern, R. J. Whitley, and B. Roizman.** 1990. Mapping of herpes simplex virus-1 neurovirulence to gamma 134.5, a gene nonessential for growth in culture. Science **250:**1262–1266.
6. **Chou, J., and B. Roizman.** 1992. The gamma 1(34.5) gene of herpes simplex virus 1 precludes neuroblastoma cells from triggering total shutoff of protein synthesis characteristic of programed cell death in neuronal cells. Proc. Natl. Acad. Sci. U. S. A. **89:**3266–3270.
7. **Cotter, C. R., et al.** 2010. The virion host shut-off (vhs) protein blocks a TLR-independent pathway of herpes simplex virus type 1 recognition in human and mouse dendritic cells. PLoS One **5:**e8684.
8. **Cozzi, P. J., et al.** 2001. Intravesical oncolytic viral therapy using attenuated, replication-competent herpes simplex viruses G207 and Nv1020 is effective in the treatment of bladder cancer in an orthotopic syngeneic model. FASEB J. **15:**1306–1308.
9. **Ding, Y., M. Tong, S. Liu, J. A. Moscow, and H. H. Tai.** 2005. NAD+-linked 15-hydroxyprostaglandin dehydrogenase (15-PGDH) behaves as a tumor suppressor in lung cancer. Carcinogenesis **26:**65–72.
10. **Eruslanov, E., et al.** 2009. Altered expression of 15-hydroxyprostaglandin dehydrogenase in tumor-infiltrated CD11b myeloid cells: a mechanism for immune evasion in cancer. J. Immunol. **182:**7548–7557.
11. **Foster, T. P., X. Alvarez, and K. G. Kousoulas.** 2003. Plasma membrane topology of syncytial domains of herpes simplex virus type 1 glycoprotein K (gK): the UL20 protein enables cell surface localization of gK but not gK-mediated cell-to-cell fusion. J. Virol. **77:**499–510.
12. **Foster, T. P., G. V. Rybachuk, and K. G. Kousoulas.** 2001. Glycoprotein K specified by herpes simplex virus type 1 is expressed on virions as a Golgi complex-dependent glycosylated species and functions in virion entry. J. Virol. **75:**12431–12438.
13. **Fukuhara, H., and T. Todo.** 2007. Oncolytic herpes simplex virus type 1 and host immune responses. Curr. Cancer Drug Targets **7:**149–155.
14. **Gabrilovich, D.** 2004. Mechanisms and functional significance of tumour-induced dendritic-cell defects. Nat. Rev. Immunol. **4:**941–952.
15. **Geevarghese, S. K., et al.** 2010. Phase I/II study of oncolytic herpes simplex virus NV1020 in patients with extensively pretreated refractory colorectal cancer metastatic to the liver. Hum. Gene Ther. **21:**1119–1128.
16. **Geiss, B. J., T. J. Smith, D. A. Leib, and L. A. Morrison.** 2000. Disruption of virion host shutoff activity improves the immunogenicity and protective capacity of a replication-incompetent herpes simplex virus type 1 vaccine strain. J. Virol. **74:**11137–11144.
17. **Greenhough, A., et al.** 2009. The COX-2/PGE2 pathway: key roles in the hallmarks of cancer and adaptation to the tumour microenvironment. Carcinogenesis **30:**377–386.
18. **Gutermann, A., et al.** 2006. Efficacy of oncolytic herpesvirus NV1020 can be enhanced by combination with chemotherapeutics in colon carcinoma cells. Hum. Gene Ther. **17:**1241–1253.
19. **Harbour, D. A., W. A. Blyth, and T. J. Hill.** 1978. Prostaglandins enhance spread of herpes simplex virus in cell cultures. J. Gen. Virol. **41:**87–95.
20. **Harizi, H., M. Juzan, C. Grosset, M. Rashedi, and N. Gualde.** 2001. Dendritic cells issued in vitro from bone marrow produce PGE(2) that contributes to the immunomodulation induced by antigen-presenting cells. Cell Immunol. **209:**19–28.
21. **Harris, R. E.** 2007. Cyclooxygenase-2 (cox-2) and the inflammogenesis of cancer. Subcell. Biochem. **42:**93–126.
22. **Harris, R. E., J. Beebe-Donk, and G. A. Alshafie.** 2007. Cancer chemoprevention by cyclooxygenase 2 (COX-2) blockade: results of case control studies. Subcell. Biochem. **42:**193–212.
23. **Harris, R. E., J. Beebe-Donk, H. Doss, and D. Burr Doss.** 2005. Aspirin, ibuprofen, and other non-steroidal anti-inflammatory drugs in cancer prevention: a critical review of non-selective COX-2 blockade (review). Oncol. Rep. **13:**559–583.
24. **Harris, S. G., J. Padilla, L. Koumas, D. Ray, and R. P. Phipps.** 2002. Prostaglandins as modulators of immunity. Trends Immunol. **23:**144–150.
25. **Israyelyan, A., et al.** 2008. Herpes simplex virus type-1(HSV-1) oncolytic and highly fusogenic mutants carrying the NV1020 genomic deletion effectively inhibit primary and metastatic tumors in mice. Virol. J. **5:**68.
26. **Israyelyan, A. H., et al.** 2007. Effective treatment of human breast tumor in a mouse xenograft model with herpes simplex virus type 1 specifying the NV1020 genomic deletion and the gBsyn3 syncytial mutation enabling high viral replication and spread in breast cancer cells. Hum. Gene Ther. **18:**457–473.
27. **Kaliberova, L. N., et al.** 2009. Experimental cancer therapy using restoration of NAD+-linked 15-hydroxyprostaglandin dehydrogenase expression. Mol. Cancer Ther. **8:**3130–3139.
28. **Kelly, K. J., J. Wong, and Y. Fong.** 2008. Herpes simplex virus NV1020 as a

novel and promising therapy for hepatic malignancy. Expert Opin. Investig. Drugs **17:**1105–1113.

29. **Kemeny, N., et al.** 2006. Phase I, open-label, dose-escalating study of a genetically engineered herpes simplex virus, NV1020, in subjects with metastatic colorectal carcinoma to the liver. Hum. Gene Ther. **17:**1214–1224.

30. **Khyatti, M., and J. Menezes.** 1990. The effect of indomethacin, prostaglandin E2 and interferon on the multiplication of herpes simplex virus type 1 in human lymphoid cells. Antiviral Res. **14:**161–172.

31. **Koziol, J. A., D. A. Maxwell, M. Fukushima, M. E. Colmerauer, and Y. H. Pilch.** 1981. A distribution-free test for tumor-growth curve analyses with application to an animal tumor immunotherapy experiment. Biometrics **37:** 383–390.

32. **Kwong, A. D., and N. Frenkel.** 1987. Herpes simplex virus-infected cells contain a function(s) that destabilizes both host and viral mRNAs. Proc. Natl. Acad. Sci. U. S. A. **84:**1926–1930.

33. **Kwong, A. D., J. A. Kruper, and N. Frenkel.** 1988. Herpes simplex virus virion host shutoff function. J. Virol. **62:**912–921.

34. **Leone, V., et al.** 2007. PGE2 inhibits apoptosis in human adenocarcinoma Caco-2 cell line through Ras-PI3K association and cAMP-dependent kinase A activation. Am. J. Physiol. Gastrointest. Liver Physiol. **293:**G673–G681.

35. **Li, M., et al.** 2008. Suppression of invasive properties of colorectal carcinoma SW480 cells by 15-hydroxyprostaglandin dehydrogenase gene. Cancer Invest. **26:**905–912.

36. **Liu, B., L. Qu, and H. Tao.** 2010. Cyclo-oxygenase 2 up-regulates the effect of multidrug resistance. Cell Biol. Int. **34:**21–25.

37. **Manservigi, R., R. Argnani, and P. Marconi.** 2010. HSV recombinant vectors for gene therapy. Open Virol. J. **4:**123–156.

38. **Marrogi, A. J., et al.** 2000. Nitric oxide synthase, cyclooxygenase 2, and vascular endothelial growth factor in the angiogenesis of non-small cell lung carcinoma. Clin. Cancer Res. **6:**4739–4744.

39. **Matzinger, P.** 1998. An innate sense of danger. Semin. Immunol. **10:**399–415.

40. **Matzinger, P.** 2002. An innate sense of danger. Ann. N. Y. Acad. Sci. **961:**341–342.

41. **Matzinger, P.** 1994. Tolerance, danger, and the extended family. Annu. Rev. Immunol. **12:**991–1045.

42. **Myung, S. J., et al.** 2006. 15-Hydroxyprostaglandin dehydrogenase is an in vivo suppressor of colon tumorigenesis. Proc. Natl. Acad. Sci. U. S. A. **103:**12098–12102.

43. **Nakamori, M., X. Fu, R. Rousseau, S. Y. Chen, and X. Zhang.** 2004. Destruction of nonimmunogenic mammary tumor cells by a fusogenic oncolytic herpes simplex virus induces potent antitumor immunity. Mol. Ther. **9:**658–665.

44. **Ochoa, A. C., A. H. Zea, C. Hernandez, and P. C. Rodriguez.** 2007. Arginase, prostaglandins, and myeloid-derived suppressor cells in renal cell carcinoma. Clin. Cancer Res. **13:**721s–726s.

45. **Oroskar, A. A., and G. S. Read.** 1989. Control of mRNA stability by the virion host shutoff function of herpes simplex virus. J. Virol. **63:**1897–1906.

46. **Ostrand-Rosenberg, S.** 2008. Immune surveillance: a balance between protumor and antitumor immunity. Curr. Opin. Genet. Dev. **18:**11–18.

47. **Ostrand-Rosenberg, S.** 2010. Myeloid-derived suppressor cells: more mechanisms for inhibiting antitumor immunity. Cancer Immunol. Immunother. **59:**1593–1600.

48. **Pasieka, T. J., et al.** 2008. Herpes simplex virus virion host shutoff attenuates establishment of the antiviral state. J. Virol. **82:**5527–5535.

49. **Prestwich, R. J., et al.** 2009. The case of oncolytic viruses versus the immune system: waiting on the judgment of Solomon. Hum. Gene Ther. **20:**1119–1132.

50. **Pulaski, B. A., and S. Ostrand-Rosenberg.** 2001. Mouse 4T1 breast tumor model. Curr. Protoc. Immunol. **Chapter 20:**Unit 20.2.

51. **Read, G. S., and N. Frenkel.** 1983. Herpes simplex virus mutants defective in the virion-associated shutoff of host polypeptide synthesis and exhibiting abnormal synthesis of alpha (immediate early) viral polypeptides. J. Virol. **46:**498–512.

52. **Read, G. S., B. M. Karr, and K. Knight.** 1993. Isolation of a herpes simplex virus type 1 mutant with a deletion in the virion host shutoff gene and identification of multiple forms of the vhs (UL41) polypeptide. J. Virol. **67:**7149–7160.

53. **Rodriguez, P. C., et al.** 2005. Arginase I in myeloid suppressor cells is induced by COX-2 in lung carcinoma. J. Exp. Med. **202:**931–939.

54. **Samady, L., et al.** 2003. Deletion of the virion host shutoff protein (vhs) from herpes simplex virus (HSV) relieves the viral block to dendritic cell activation: potential of vhs⁻ HSV vectors for dendritic cell-mediated immunotherapy. J. Virol. **77:**3768–3776.

55. **Santos, F. C., et al.** 2006. Seroepidemiological study of herpes simplex virus type 2 in patients with the acquired immunodeficiency syndrome in the city of Niteroi, Rio de Janeiro, Brazil. Mem. Inst. Oswaldo Cruz **101:**315–319.

56. **Schek, N., and S. L. Bachenheimer.** 1985. Degradation of cellular mRNAs induced by a virion-associated factor during herpes simplex virus infection of Vero cells. J. Virol. **55:**601–610.

57. **Sharma, S., et al.** 2005. Tumor cyclooxygenase-2/prostaglandin E2-dependent promotion of FOXP3 expression and CD4+ CD25+ T regulatory cell activities in lung cancer. Cancer Res. **65:**5211–5220.

58. **Sinha, P., V. K. Clements, A. M. Fulton, and S. Ostrand-Rosenberg.** 2007. Prostaglandin E2 promotes tumor progression by inducing myeloid-derived suppressor cells. Cancer Res. **67:**4507–4513.

59. **Smiley, J. R.** 2004. Herpes simplex virus virion host shutoff protein: immune evasion mediated by a viral RNase? J. Virol. **78:**1063–1068.

60. **Smith, T. J., L. A. Morrison, and D. A. Leib.** 2002. Pathogenesis of herpes simplex virus type 2 virion host shutoff (vhs) mutants. J. Virol. **76:**2054–2061.

61. **Sorenson, C. M., P. A. Hart, and J. Ross.** 1991. Analysis of herpes simplex virus-induced mRNA destabilizing activity using an in vitro mRNA decay system. Nucleic Acids Res. **19:**4459–4465.

62. **Strelow, L., T. Smith, and D. Leib.** 1997. The virion host shutoff function of herpes simplex virus type 1 plays a role in corneal invasion and functions independently of the cell cycle. Virology **231:**28–34.

63. **Strelow, L. I., and D. A. Leib.** 1996. Analysis of conserved domains of UL41 of herpes simplex virus type 1 in virion host shutoff and pathogenesis. J. Virol. **70:**5665–5667.

64. **Strelow, L. I., and D. A. Leib.** 1995. Role of the virion host shutoff (vhs) of herpes simplex virus type 1 in latency and pathogenesis. J. Virol. **69:**6779–6786.

65. **Strom, T., and N. Frenkel.** 1987. Effects of herpes simplex virus on mRNA stability. J. Virol. **61:**2198–2207.

66. **Tai, H. H., M. Tong, and Y. Ding.** 2007. 15-hydroxyprostaglandin dehydrogenase (15-PGDH) and lung cancer. Prostaglandins Other Lipid Med. **83:** 203–208.

67. **Tatsuwaki, H., et al.** 2010. Reduction of 15-hydroxyprostaglandin dehydrogenase expression is an independent predictor of poor survival associated with enhanced cell proliferation in gastric adenocarcinoma. Cancer Sci. **101:**550–558.

68. **Tischer, B. K., J. von Einem, B. Kaufer, and N. Osterrieder.** 2006. Two-step red-mediated recombination for versatile high-efficiency markerless DNA manipulation in Escherichia coli. Biotechniques **40:**191–197.

69. **Trgovcich, J., D. Johnson, and B. Roizman.** 2002. Cell surface major histocompatibility complex class II proteins are regulated by the products of the gamma(1)34.5 and U(L)41 genes of herpes simplex virus 1. J. Virol. **76:**6974–6986.

70. **Tseng-Rogenski, S., et al.** 2010. Loss of 15-hydroxyprostaglandin dehydrogenase expression contributes to bladder cancer progression. Am. J. Pathol. **176:**1462–1468.

71. **Tsujii, M., et al.** 1998. Cyclooxygenase regulates angiogenesis induced by colon cancer cells. Cell **93:**705–716.

72. **Wacholtz, M. C., R. Minakuchi, and P. E. Lipsky.** 1991. Characterization of the 3′,5′-cyclic adenosine monophosphate-mediated regulation of IL2 production by T cells and Jurkat cells. Cell. Immunol. **135:**285–298.

73. **Wanebo, H. J., R. Pace, S. Hargett, D. Katz, and J. Sando.** 1986. Production of and response to interleukin-2 in peripheral blood lymphocytes of cancer patients. Cancer **57:**656–662.

74. **Yan, M., et al.** 2004. 15-Hydroxyprostaglandin dehydrogenase, a COX-2 oncogene antagonist, is a TGF-beta-induced suppressor of human gastrointestinal cancers. Proc. Natl. Acad. Sci. U. S. A. **101:**17468–17473.

75. **Zelus, B. D., R. S. Stewart, and J. Ross.** 1996. The virion host shutoff protein of herpes simplex virus type 1: messenger ribonucleolytic activity in vitro. J. Virol. **70:**2411–2419.

76. **Zou, W.** 2005. Immunosuppressive networks in the tumour environment and their therapeutic relevance. Nat. Rev. Cancer **5:**263–274.